STM JOURNALS

Journal of
Polymer & Composites

https://journals.stmjournals.com/JOPC/

ISSN: 2321-2810 (Online)
ISSN: 2321-8525 (Print)
Volume 12, Special Issue 6, 2024
DOI (Journal): 10.37591/JoPC

Research JoPC

Experimental Evaluation of MDM@Gd_2O_3:Eu^{3+} and Protein@MDM@Gd_2O_3:Eu^{3+} Functional Nanomaterial

Ashutosh Sharma[1], Dinesh Sharma[2,*], Richa Singh[3]

Abstract

Lanthanide cation like Eu^{3+} (europium Xe $4f^6 6s^0$) doped functional nanomaterials of lanthanide oxides especially of gadolinium oxide (Gd_2O_3) as nanorods capped with monodispersed macromolecule (MDM) like polyvinylpyrrolidone (PVP) coated with natural biopolymers like proteins as human serum albumin (HSA) have been the most demanding and applied nanomaterials in areas of the biosensor, optical distinguisher, electronic fluoresces, upconversion, and surface plasmonic resonance (SPR) nanomaterials and others. The Gd^{3+} and Eu^{3+} lanthanide cations with $4f^7$ and $4f^{3+}$ electrons in their 4f shells have been chosen for studies in this study. These cations have almost similar contraction activities with almost similar Fermi energy barriers.The closely placed electrons in their 4f shells have produced the thermodynamic and kinetic colloidal stability of the PVP@Gd_2O_3:Eu^{3+} and HSA@PVP@Gd_2O_3:Eu^{3+} functional nanomaterials due to stoichiometrically balanced oxidation potentials, hydrophobicity, and electrostatic dipoles. Various composite materials have been produced using natural fibers through adapted synthetic techniques, broadening their potential applications from automotive to biomedical sectors. Sisal, coconut, eucalyptus pulp, jute, bamboo, malva, hemp, banana, pineapple leaf, ramie bast, kenaf bast, flax, sugarcane fiber, date palm, and cotton are commonly utilized as natural reinforcements in polymer composites to enhance desired properties.

Keywords: Nanorods, nanomaterial's, capping, coating, colloidal stability, fermi energy

INTRODUCTION

Advanced composites are widely favored across various engineering applications due to their exceptional specific strength and specific stiffness, offering superior performance relative to their weight. Within the aircraft and aerospace industries, high-strength fibers such as carbon, glass, and Kevlar are commonly employed. These fibers contribute robust tensile strength essential for supporting both tensile and bending stiffness within composite structures. Polymer-based matrices play a crucial role in these composites by acting as a protective layer for the high-strength, brittle fibers, particularly against impacts. Moreover, the matrix material serves to absorb vibrational energy, enhancing the structural integrity of rigid components, particularly in safeguarding against seismic disturbances. Currently, nanoscience and technology of the lanthanide-doped, lanthanide oxide nanomaterials capped with biocompatible monodispersed polymer molecules like PVP (Baqer *et al.*, 2017) [2]. PEG(Bridot *et al.*, 2007)[5],alkanethiols of variable alkyl chains (Azubel *et al.*, 2016[1]: Battocchio *et al.*, 2014) [3]. and dendrimer (Zhao *et al.*, 2014) [49]. like TTDMM (trimesyol-1,3,5-trimethyl malonate), TSMM (Trisurfactantomethylol melamine), and Tri-o-tolyl benzene-1,3,5-tricarboxylate (TOBT), tri-4-hydroxyphenyl benzene-1,3,5-tricarboxylate (THBT), and tri-3,5- dihydroxyphenyl benzene - 1,3,5-tricarboxylate (TDBT) have been the most

***Author for Correspondence**
Dinesh Sharma

[1]Associate Professor, Department of Chemistry, Arya College of Engineering and I.T, Jaipur, Rajasthan, India
[2]Assistant Professor, Department of Chemistry, Poornima College of Engineering Jaipur, Rajasthan, India
[3]Associate Professor, Department of Chemistry, Arya College of Engineering and I.T, Jaipur, Rajasthan, India

Received Date: April 01, 2024
Accepted Date: April 09, 2024
Published Date: September 30, 2024

Citation: Ashutosh Sharma, Dinesh Sharma, Richa Singh. Experimental evaluation of MDM@Gd_2O_3:Eu^{3+} and protein@MDM@Gd_2O_3:Eu^{3+} functional nanomaterial. Journal of Polymer & Composites. 2024; 12(Special Issue 6): S214–S.223

desirable sensors. . The utilization of natural fibers as reinforcing agents for polymer composites is progressively increasing in engineering applications. Various composite materials have been produced using natural fibers through adapted synthetic techniques, broadening their potential applications from automotive to biomedical sectors. Sisal, coconut, eucalyptus pulp, jute, bamboo, malva, hemp, banana, pineapple leaf, ramie bast, kenaf bast, flax, sugarcane fiber, date palm, and cotton are commonly utilized as natural reinforcements in polymer composites to enhance desired properties. The mechanical properties of cellulosic fibers are influenced by factors such as specific gravity, length, diameter, processing techniques, and treatment, which play a significant role in determining their potential applications. Additionally, there are several underexplored fibers like henequen, esparto, hibiscus sabdariffa, sabai grass, and pines, which possess significant potential in terms of thermal resistance, chemical constituents, and mechanical properties comparable to bamboo, hemp, jute, and oil palm fibers. Construction materials and techniques focus on enhancing the functional properties of glass, steel, concrete, and wood, which are fundamental for construction purposes. They offer cost-effectiveness compared to composite materials, especially when a significant proportion of fibers is employed, as opposed to steel fibers. The incorporation of natural fibers in construction promotes a more environmentally friendly, sustainable, and intelligent approach compared to polymer, steel, or synthetic fibers. Capping NPs with biocompatible/organic macromolecules increases dispersion, stability and decreases nonspecific interactions with cells and proteins and reduces their toxicity (Charbgoo *et al*., 2017) [8]. The capped lanthanide oxide nanoparticles coated with various proteins (Que *et al.,* 2017) [35]. lipoproteins constitute remarkable biophysics, biomedical, and bioengineer sciences. Such materials develop the potential interfaces among the structural molecules as well as their physicochemical properties which become an asset for several functions in the material sciences (Mahmoudi *et al.,* 2011) [31]. Lanthanide oxide (Ln_2O_3) nanomaterials have gathered considerableinterest among the scientific communitydue to their outstanding optical and electronic properties (Boopathi *et al.,* 2017) [4]. They have marked applications such as high energy radiation detectors (Hase *et al.,* 1990) [20]. luminescent devices (Tissue *et al.,* 1986;) [41]. biomarkers (Lechevallier *et al.,* 2010) [25]. panel displays (Das *et al.,* 2010) [12]. optical data storage (Chen *et al.,* 2016) [10]. drug carriers (Zhang *et al.,* 2015) [48]. etc.They are used as fluorescent labelling agents because of long luminescence lifetimes, large stoke shifts, photostabilities and narrow emission properties (Gordon *et al.,* 2004[17]. Sun *et al.,* 2016) [40].The Gd_2O_3 NPs are of significant use due to their proton relaxation, low phonon energy (Xiao *et al.[45],* 2009; Louis *et al.,* 2005)[29] and scintillation properties like CT scan (Cha *et al.,* 2011[7]. Vashistha *et al.,* 2018) [43]. respectively.The luminescenceapplications of Gd_2O_3 are due to f–f transitions of half-filled 4f shell (Bunzli *et al.,* 2010[6]; Hansen *et al.*,2013) [19]. These transitions are forbidden in nature and havelow molar absorptivity values of Gd_2O_3(Stouwdam *et al.,* 2002[39]; Luo *et al.,* 2009) [30]. Such limitationsareresolvedby low atom percentdoping of the Gd_2O_3 with lanthanide ion (Ln^{3+}) like Eu^{3+}(Ghosh and Luwang 2015; Ghosh and Luwang 2015; Ghosh and Luwang 2016) [13-15]. The Eu^{3+} doped Gd_2O_3 absorb light effectively and transfer it to Gd^{3+} ion withenhanced emission (Han *et al.,* 2014[18]; Zhang *et al.,* 2007) [47]. Eu^{3+} due to its higher effective absorption and lower diffusion barrier (Liu *et al.,* 2010[28]; Nichkova *et al.,* 2005) [32]. used as an potential dopant with various specific applications.These have applications in biological fluorescent labels (Nichkova *et al.,* 2007) [33]. contrast agents (Goldys *et al.,* 2006) [16]. and display applications (Zhou *et al.,* 2003[50]; Rossner *et al.,* 1991) [36]. The effects of proteins like BSA or HSA functionalized PVP@Gd_2O_3:Eu^{3+} NPs surfaces on fluorescence detection of transition metal ions compared to PVP@Gd_2O_3:Eu^{3+} NPs in aqueous (aq.) have investigated the novel theory and understanding in field of detection chemistry of transition metal ions which could be extended to other useful materials. To optimize the stability of doped NPs we have calculated the electronic energies of both the host and the dopant ions using Fermi-Dirac equation (Cranstoun *et al.,* 1984) [11].

$$(E - E_f) = K_B T \ln[1/\ f(E,T) - 1] \quad .29$$

The E isthe energy of particle or electron of 4f orbital of Gd^{3+} and Eu^{3+}, E_F is Fermi energy, f is particle fraction, k_B is Boltzmann distribution constant, T is the temperature in kelvin. The electronic energies ($E-E_f$) at T=298 K calculated for $4f^7$ (Gd^{3+}) and $4f^6$ (Eu^{3+}) electrons are 7.67×10^{-2} eV and

7.60×10^{-2} eV for Gd^{3+} and Eu^{3+} respectively. Thus, the Fermi energy is temperature dependent because the electrons gain kinetic energy out of the temperature and get oscillated within certain energy orbits. Thus, the colloidalstability is also controlled and tuned by the electronicoscillationwhereas the electron oscillation itself isa function of the temperature. There have been a few reports on heavy metal ion detection in water using Ln doped NPs but no systematic detection mechanism is explored yet (Li *et al.*, 2013 [26]. Sarkar *et al.*,2014) [37]. Detection of Fe^{3+}, Cr^{3+}, Cu^{2+} ionsin drinking water and other industrial formulations is highly significant as these are essential trace elements and their anomalies may cause various abnormalities in human health (Wang *et al.*, 2014[44]. Zhou *et al.*, 2008[51]. Ye *et al.*, 2015) [46]. The Gd^{3+} based functional nanomaterials performing as high-efficiency T1 contrast agents providing a positive signal, makes them the extensively used contrast agents in magnetic resonance imaging (MRI) for safer detection (Chen *et al.*,2011[8]. Hifumi *et al.*, 2006) [21]. GdF_3 or $NaGdF_4$ could be doped with other lanthanide ions to combine optically and MR contrast effects into dual modality probes (Park *et al.*, 2009[34]; Ju *et al.*, 2011) [24]. In recent years, Gd_2O_3-Eu^{3+} NPs were synthesized by different techniques due to excellent properties and broad applications. Jain and Hirata have studied the influence of various types of synthetic methodologies on the preparation of Gd_2O_3-Eu^{3+} NPs and their luminescence activities [Jain & Hirata 2016][22]. The effect of doping and co-doping strategies over Gd_2O_3 NPs have been carried out to investigate luminescence efficiency of prepared particles (Lin *et al*., 2016) [27]. Zou and co-workers prepared the templating of Gd_2O_3-Eu^{3+} NPs with polymers to introduce the hydrophilicity to the prepared NPs, which further affect the photoluminescence properties of Gd_2O_3-Eu^{3+} NPs as their efficient employment in adsorption studies [Zoua *et al*., 2017] [52]. Gd_2O_3-Eu^{3+} NPs have also been used for the dual-modal fluorescence and MRI agents with excellent efficiency as drug delivery agent [Shi *et al*., 2015][38]. Tuo and co-workers have used the application of magnetic NPs over Gd_2O_3-Eu^{3+} NPs for enhancing their applications in targeted drug delivery or luminescent labels [Tuo *et al*., 2016][42]. Due to the increased role of Gd_2O_3-Eu^{3+} NPs in diagnostics encouraged Jin et al. to study the cytotoxic effect of Eu doped Gd_2O_3 NPs on the bone marrow stromal cells [Jin *et al*., 2015] [23]. Thus, thiswork opens a new window for several other possibilities for designing several functional nanomaterials like AT@Gd_2O_3:Eu^{3+}, AT is alkanethiol, TTDMM@Gd_2O_3:$Eu^{3+}$with respective BSA@AT@Gd_2O_3:Eu^{3+} and BSA@TTDMM@Gd_2O_3:Eu^{3+} proteins coated nanomaterials.

MATERIALS AND METHODS

Reagent and Materials

The chemicals which were used were of analytical reagent grades and were used as received. Before solution preparation, they were dried at 303.15 K for 3h and kept over anhydrous calcium chloride in a vacuum desiccator for ~72h. The Millipore water was used for solutions preparations and other required precautions were taken to get high reproducibility and accuracy.

Synthesis of Nanoparticles

Thereby it has been the efforts to develop the nanoparticle which could have tuned or the controlled oscillatory motions, rotational or electronic or vibrational motionswhich are expressed as tentropy through the friccohesity of the liquid mixtures. These motions lead to develop the coagulation and clusterization that form the bulk materials in place of the nanoparticles. Thus, the for PVP@Gd_2O_3:Eu^{3+} NPs synthesis, to 30 mL (0.33 M) aq-$Gd(NO_3)_3$, the 30 mL(1 M) aq-NaOH was added dropwise on stirring. It had formed the $Gd(OH)_3$ suspension, which was centrifuged at 6000 rpm with repeated washings with water neutralization of pH. Later the $Gd(OH)_3$ and $Eu(NO_3)_3$ (10mol %) were transferred to 250 mL RB flask where 30 mL water was added with stirring until it get dispersed. To this another solution containing 1g PVP, 1g urea, and 20 mL of 30% H_2O_2 was added slowly on stirring. The mixture was then refluxed at 90°C for 48 h, with addition of 10 mL 30% H_2O_2 after every 8 h of interval. The PVP@Gd_2O_3:Eu^{3+} NPs was centrifuged at 8000 rpm for 20 min and repeatedly washed with 50% aq. ethanol to remove the unreacted PVP and urea. NPs were dried at 50°C for 12 h in a vacuum oven and stored.For preparation of HSA functionalised PVP@Gd_2O_3:Eu^{3+} NPs (HSA@PVP@Gd_2O_3:Eu^{3+} NPs),20 mg of PVP@Gd_2O_3:Eu^{3+} NPs were dispersed in 20 mL aq. HSA with stirringfor 2 h, for HSA

adsorption on PVP@Gd_2O_3:Eu^{3+} NPs surfaces. The HSA@PVP@Gd_2O_3:Eu^{3+} NPs were thencentrifuged at 8000 rpm for 20 min with repeated washings with Milli-Q water. HSA@PVP@Gd_2O_3:Eu^{3+} NPs were dried in a vacuum oven at 25°C for 12 h and stored.

Characterisations and Instrumentation

For morphology study of PVP@Gd_2O_3:Eu^{3+} and HSA@PVP@Gd_2O_3:Eu^{3+} NPs, HR-TEM was performed using a JEOL JEM-2100 HR-TEM, at 180 kV. Quantitative estimation of metal ions in water samples was done in triplicate on ICP-OES (7300DV, Perkin Elmer) instrument.

RESULTS AND DISCUSSION

Nanoemulsions are developed through the colloidal states of the ingredients in the specified mixture of the chemical species. These species have electrostatic, hydrophilic, hydrophobic and a localized shift the sheared electron pair. These electrostatics developed the nanohydration spheres (NHS) and sometimes the micelles when the prominent surfactants are present but in this study no surfactants are added excepting capping the Gd_2O_3:Eu^{3+} with PVP and coating with the proteins. Hence no free alkyl chains exit but the hydrophobic parts are also engaged. Thus, there is a prominent possibility to develop the NHS. Thereby the NHS seem the most dynamics arrangements of the chemical species to develop stable colloids. Thermodynamic and kinetic stability of PVP@Gd_2O_3:$Eu^{3+}$and protein@PVP@Gd_2O_3:Eu^{3+} NPs is the most critical index to use them for tuning the chemical and biochemical properties of the desired biochemically important species. The PVP@Gd_2O_3:Eu^{3+} and protien@PVP@Gd_2O_3:Eu^{3+} NPs have lanthanide cations with electronically contraction and biocompatible PVP and HSA macromolecules respectively which respond to ionic strength and pH of water, DMEM, and RPMI media. The Eu^{3+} with $4f^6$ electrons is doped with Gd^{3+} of Gd_2O_3 LNR with $4f^7$ electrons where the repulsion Gd^{3+} between Eu^{3+} is optimized due to electronegative O atoms of Gd_2O_3. A poor shielding of nuclear charges of Gd^{3+} and Eu^{3+} with stronger nuclear attractive force of their 4f electrons as the 6s electrons move towards the nucleus. The Gd^{3+} and Eu^{3+} with multi-electrons lower their radius on increasing electrostatic repulsion among their electrons. Therefore, their poor shielding effect with a lower effective charge on their nucleus could leach out the Eu^{+} in liquid medium. The media DMEM and RPMI both have salts along with 13 amino acids, and 8 vitamins: thiamine (vitamin B_1), riboflavin (vitamin B_2), nicotinamide (vitamin B_3), pantothenic acid (vitamin B_5), pyridoxine (vitamin B_6), folic acid (vitamin B_9), choline, and myo-inositol (vitamin B_8). Thereby, due to a shielding effect exerted by inner electrons decreases in $s > p > d > f$ order, it could be developed stronger cation-cation interactions to ensure their stabilities the samples were kept for 24 and 48 h but no change was noticed which confirmed the thermodynamic and kinetic stability. Therefore PVP@Gd_2O_3:Eu^{3+} and HSA@PVP@Gd_2O_3:Eu^{3+} NPs could be used for detections of wider numbers of metallic, metal complex and other formulation holding active metallic ions under various experimental conditions like variable pH and temperatures. The TGA also supported high stabilities of these NPs. This proves that the Eu^{3+} is accommodated within the Gd_2O_3 unit with exceptionally strong ionic forces. The PVP and HSA also capped through stronger van der Waals forces which might have developed a synergy among the peptide bonds of the HSA and the pyrrolidone ring of the PVP with equipartition of their electronic energies depicted with the following equation.

The E is energy of a particle and E_F is fermi energy, $k_B$is Boltzmann distribution constant (k_B =1.38065×$10^{-23}$$JK^{-1}$), f is particle fraction, T is kelvin temperature, E is energy. The energy for $4f^7$ and $4f^6$ electrons is calculated as.

$$\left(E - E_F\right) = \mathrm{k_B T ln}\left(\frac{1}{7} - 1\right)$$

The (E-E_F) which is Fermi energy is 63.4675×10^{-23} JK^{-1} for Gd^{3+} and the 75.06618×$10^{-23}$$JK^{-1}$ is for Eu^{3+}which are closer to each other. Therefore, the combination of the Gd^{3+} and the $Eu^{3+}$for developing the PVP@Gd_2O_3:Eu^{3+} and protien@PVP@Gd_2O_3:Eu^{3+} NPs possible and is fermi energy -wise is stable that develop the minimum interfacial energy between the contraction of these lanthanide cations. The oxidation potentials of the Gd_2O_3 and Eu^{+} differ because of the negative oxidation potential or the reduction potential of the electronegative O atoms bonded with the Gd_2O_3 NPs which might have developed the interfacial energy. This energy could be responsible for capping with the PVP and coating with proteins. Therefore, these interfacial sciences of the PVP@Gd_2O_3:Eu^{3+} and

protien@PVP@Gd_2O_3:Eu^{3+} NPs don't allow them for coagulation or clusterization. Since the PVP, proteins, Gd_2O_3, and Eu^{+} have different electronic environments that develop variable Lennard Jones potential energy wells and hence as per Born-Oppenheimer approximation the electron – nuclei attractions, nuclei – nuclei and electron – electron repulsion occur. These electronic activities of the PVP@Gd_2O_3:Eu^{3+} and protien@PVP@Gd_2O_3:Eu^{3+} NPs make them the most unique chemical species for developing the friccohesities in species solvent media. Thus, to test the durability of the expression of the friccohesity of the NPs, the sample were kept for a certain time duration without shaking the samples.

Therefore, no coagulation, flocculation, aggregation, sedimentation occur for 48h which an extraordinary stability of PVP@Gd_2O_3:Eu^{3+} and HSA@PVP@Gd_2O_3:Eu^{3+} NPs. The texture, surface area, particle size, shear stress, surface energy, and cohesive energy didn't undergo charges with time. Thus, the PVP@Gd_2O_3:Eu^{3+} and HSA@PVP@Gd_2O_3:Eu^{3+} NPs both have higher surface area with least activation as these were remained monodispersed in aqueous solutions for a longer time i.e. 48h (shceme1). This is the reason that these NPs have highest detection resolutions and accuracies. The work is continued to dope the Gd_2O_3 with Sm^{3+}, Pr^{3+} with variable electrons in the 4f shells.

Figure 1. shows the interacting interfaces of the constitutional units which have specific electronic charge clouds, acting as a driving forces to generate the stability of the PVP@Gd_2O_3:Eu^{3+} and HSA@PVP@Gd_2O_3:Eu^{3+} NPs. The interfaces infers adequate charges and electrostatic potential or linkages that seem responsible for the stacking of NRs (nanorods) due to the terminal linkages. Therefore PVP@Gd_2O_3:Eu^{3+} develop significant geometrical spatial interfaces as the functional nanorods. The interlinked grooves are visible in the Figure 1 which are developed due to the interacting interfacial points causing flattening of the NRs. The NPs of HSA@PVP@Gd_2O_3:Eu^{3+} are also rod shaped, where the rough edges and surfaces are smoothened with HSA coating. This proves that the interfaces are fitted with HSA as it has polar peptide bonds. Thus, the surfaces of HSA@PVP@Gd_2O_3:Eu^{3+} are comparatively defined with almost even and smooth surfaces. Thus, the HSA is equally distributed over the surfaces of PVP@Gd_2O_3:Eu^{3+}. This may be supported with the negative potential of the O^{2-} and the positive potential of the Gd^{3+}, Eu^{3+} and the hydrophobicity of the PVP has attracted the HSA towards the PVP@Gd_2O_3:Eu^{3+}. Taking a note of the HR-TEM images depicted in Figure 2, the image of bare Gd_2O_3:Eu^{3+} NPs demonstrates a reduced particle size after annealing of PVP@Gd_2O_3:Eu^{3+}NPs, due to a removal of a PVP layer. Also, the annealed bare PVP@Gd_2O_3:Eu^{3+} NPs are comparatively sharper, thinner and pointed which depict that the PVP has regulated the NRs otherwise these had been closely placed NRs with sharper ends. Clustering due to HSA coating is observed in HR-TEM images of HSA@PVP@Gd_2O_3:Eu^{3+} NPs, probably due to a presence of weak van der Walls forces between the NPs. The PVP assisted surface modification of PVP@Gd_2O_3:Eu^{3+}NPs by HSA is depicted in Figure 1.

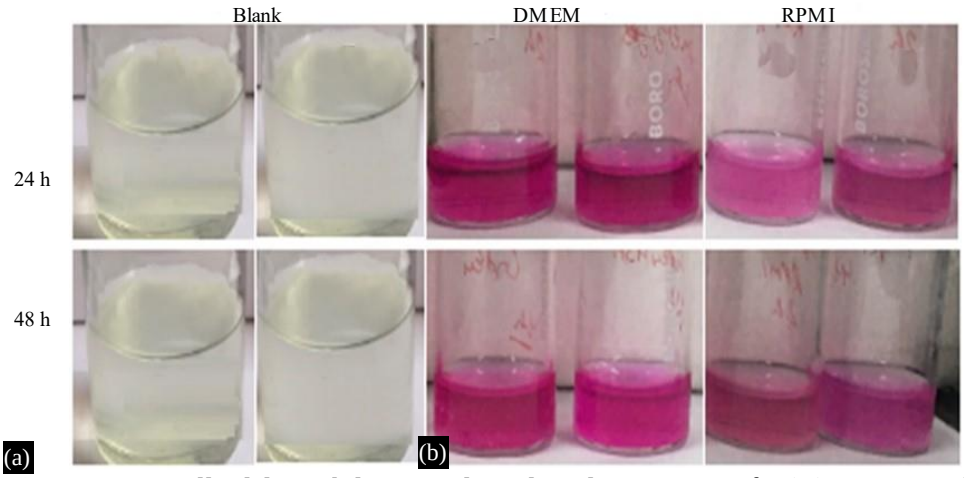

Figure 1. Colloidal stability study: digital images of (A) PVP@Gd_2O_3:Eu^{3+} and (B) HSA@PVP@Gd_2O_3:Eu^{3+} NPs after incubation in different biological media for 48h.

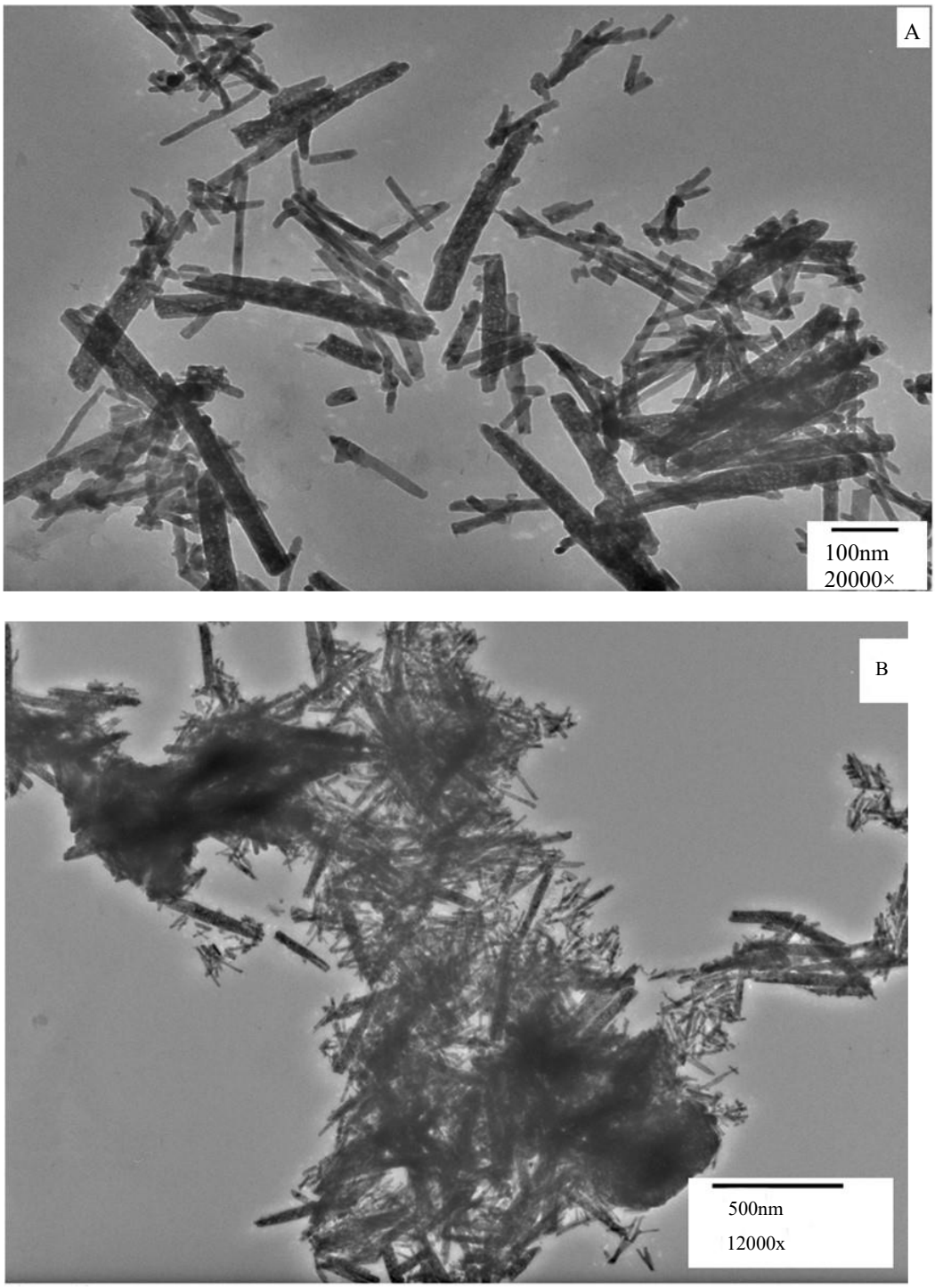

Figure 2. HR-TEM images of (A) PVP@Gd_2O_3:Eu^{3+} NPs (B) HSA@PVP@Gd_2O_3:Eu^{3+} NPs.

Fundamentally the PVP molecule which pyrrolidone ring attached with longer alkyl chain seems to spatially surround and develops the nano-thin film around the Gd_2O_3:Eu^{3+} NPs where the NRs thickened and elongated (Figures.1A and B). probably the PVP seems to be tuned by the difference in the oxidation potential of the $2Gd^{3+}$ and the reduction potential of the $3O^{2-}$ where the Eu^{3+} could also be fitted as it has oxidation potential like the Gd^{3+}. Therefore, the NRs are of 100 nm and which express the interlinked becausethe areas are darkened or staked but rest of the areas of the NRs are comparatively dim or the lighter in density. Therefore, the darker or the lighter dot or intensified areas packed on the NR outer surfaces area infer that linkages noted as under.

Figure.3 shows that the stacking and elongation mechanism is possible through of the negative and positive oxidation potentials of and O atoms and the lanthanide cations. Their networking develops the charges deficient and charge rich areas where the Eu^{3+} cations are doped. There fore, the PVP also makes a thin film around them the topological structure is developed through alignments of the several charges. The proteins like BSA or HSA both coat the PVP@Gd_2O_3:Eu^{3+} NPs as HSA@PVP@Gd_2O_3:Eu^{3+} NPs, where the PVP hydrophobicity structure assists the proteins alpha and beta sheets to deconvolute and undergo certain charges to coat the NPs.There fore, the PVP constituents synergize with the protein constituents where the key control is made by the lanthanide cations within their structural frameworks (Figure.3). The PVP structured which longer alkyl chains and the pyrrolidone ring is depicted below.

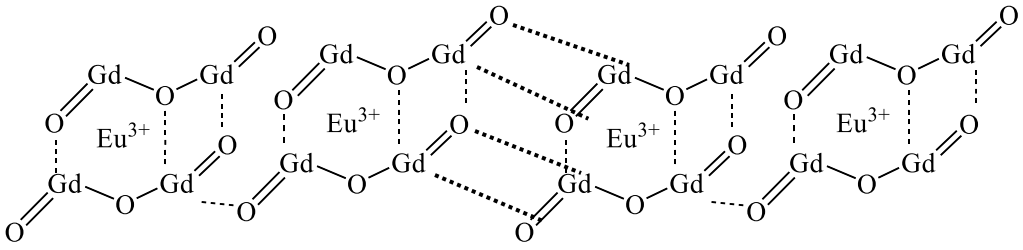

Figure 3. Stacking and elongation in 1D of NRs.

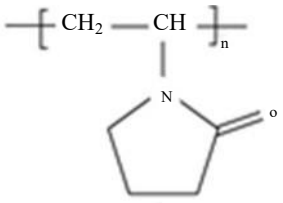

Polyvinylpyrrolidone

Probably the HSA also affect the elongation of the NRs because with HSA coating the size is narrowed down and with more lengths.

CONCLUSION

The oxidation potentials of the Gd_2O_3 and the Eu^{3+} operate for the doping and for the capping with the PVP molecules. The lanthanide nanorods are interconnected through the O atoms of one unit with the Gd cation of other units due to their opposite charges. Their charges also operate to coat the with proteins. Therefore, the PVP@Gd_2O_3:Eu^{3+} NPs as HSA@PVP@Gd_2O_3:Eu^{3+} NPs with innumerable opposite and unequal charges centers develop stable nanocolloids.

Acknowledgements

Authors acknowledge Defence Research and Development Organization (DRDO), Government of India (Research project No. ERIP/ER/1203062/M/01/1586), for financial assistance. The authors are thankful to Central University of Gujarat, Gandhinagar for infrastructural support.

REFERENCES

1. Azubel, M., & Kornberg, R. D. (2016). Synthesis of Water-Soluble, Thiolate-Protected Gold Nanoparticles Uniform in Size, Nano Letters, 16, 3348-3351
2. Baqer, A. A., Matori, K. A., Al-Hada, N. M., Shaari, A. H., Saion, E., & Chyi, J. L. Y. (2017). Effect of polyvinylpyrrolidone on cerium oxide nanoparticle characteristics prepared by a facile heat treatment technique, Results in phys.
3. Battocchio, C., Porcaro, F., Mukherjee, S., Magnano, E., Nappini, S., Fratoddi I., Quintiliani, M., Russo, M. V., & Polzonetti, G. (2014). Gold Nanoparticles Stabilized with Aromatic Thiols: Interaction at the Molecule–Metal Interface and Ligand Arrangement in the Molecular Shell Investigated by SR-XPS and NEXAFS, The Journal of Physical Chemistry C, 118, 8159-8168.

4. Boopathi, G., Raj, S.G., Kumar, G.R., Mohan, R., & Mohan, S. (2017). Synthesis of samarium doped gadolinium oxide nanorods, its spectroscopic and physical properties. Indian J Phys., 92 (6), 715-724.
5. Bridot, J.-L., Faure, A.-C., Laurent, S., Rivière, C., Billotey, C., Hiba, B., Janier, M., Josserand V, Coll, J. L., Elst L. V., Muller, R., Roux, S., Perriat, P. & Tillement, O. (2007). *Hybrid Gadolinium Oxide Nanoparticles: Multimodal Contrast* Agents for in Vivo Imaging J. AM. CHEM. SOC. 2007, 129, 5076-5084
6. Bunzli, J-C. G. (2010). Lanthanide Luminescence for Biomedical Analyses and Imaging, Chem. Rev, , 110, 2729–2755.
7. Cha, B. K., Muralidharan, P., Lee, S. J., Kim, D. K., Cho, G., & Jeon, S. (2011). Hydrothermal synthesis, structure and scintillation characterization of nanocrystalline Eu3 doped Gd2O3 materials and its X-ray imaging applications, NuclInstr Methods Phys Res Sect A Accel Spectrom. Detect Assoc Equip., 652, 212–5.
8. Charbgoo, F., Bin Ahmad, M., Darroudi, M. (2017). Cerium oxide nanoparticles: green synthesis and biological applications. Int J Nanomedicine. Dove Press, 12, 1401.
9. Chen, F., Bu, W. B., Zhang, S. J., Liu, X. H., Liu, J. N., & Xing, H. Y. (2011). Positive and negative lattice shielding effects co-existing in Gd(III) ion doped bifunctional upconversion nanoprobes, Adv Funct Mater., 21, 4285-4294.
10. Chen, J., Guo, C., & Li, T. (2016). A multicolor emitting single phase phosphor Ba3LaNa(PO4)3F:Eu2+, Pr3+ for plant growth light-emitting diodes, Sci. Adv. Mater., 8, 1374–1380.
11. Cranstoun, G. K. L., Egdell, r. G., Hill, M. D., & Samson, R. (1984). Direct observation of fermi-dirac distribution of Conduction electrons in ruthenium: a photoemission Study, J. Electron Spectrosc. Relat. Phenom., 33, 23-27
12. Das, G.K., Heng, B.C, Ng, S.C., White, T., Loo, J.S.C., D'silva, L., Padmanabhan, P., Bhakoo, K. K., Selvan S.T., & Tan, T.T.Y. (2010). Gadolinium oxide ultranarrow nanorods as multimodal contrast agents for optical and magnetic resonance imaging. Langmuir, 26, 8959–8965.
13. Ghosh, D., & Luwang, M. N. (2015). One-pot Synthesis of 2-thenoyltrifluoroacetone Surface Functionalized SrF2:Eu3+ Nanoparticles, RSC Adv., 5, 47131-47139.
14. Ghosh, D., & Luwang, M. N. (2015). p-Aminobenzoic acid (pABA) sensitization of LaF3:Tb3+ nanoparticles and its applications in the detection of explosive materials. RSC Adv., 5, 10468-10478.
15. Ghosh, D., & Luwang, M. N. (2016). Selective detection of Fe3+, Cr3+ and Cu2+ in water using highly luminescent Gd2O3:Eu3+ nanoparticles, J. Lumin., 171, 1-8.
16. Goldys, E. M., Tomsia, K. D., Jinjun, S., Dosev, D., Kennedy, I. M., Yatsunenko, S., & Godlewski, M. (2006). Optical Characterization of Eu-Doped and Undoped Gd2O3 Nanoparticles Synthesized by the Hydrogen Flame Pyrolysis Method, J. Am. Chem. Soc., 128,14498-14505.
17. Gordon, W.O., Carter, J.A., & Tissue, B.M. (2004). Long-lifetime luminescence of lanthanide-doped gadolinium oxide nanoparticles for immunoassays,. J. Lumin., 108, 339–342.
18. Han, S., Deng, R., Xie, X., & Liu, X. (2014). Enhancing Luminescence in Lanthanide-Doped Upconversion Nanoparticles, Angew. Chem. Int. Ed., 53, 11702–11715.
19. Hansen, P. A., Fjellvåg, H., Finstadband T., & Nilsena, O. (2013). Structural and optical properties of lanthanide oxides grown by atomic layer deposition (Ln = Pr, Nd, Sm, Eu, Tb, Dy, Ho, Er, Tm, Yb), Dalton Trans., 42, 10778–10785.
20. Hase, T., Kano, T., Nakazawa E., & Yamamoto, H. (1990). Phosphor materials for cathode-ray tubes. Adv. Electron. Electron. Phys., 79, 271-373.
21. Hifumi, H., Yamaoka, S., Tanimoto, A., Citterio, D., & Suzuki, K. J. (2006). Gadolinium-based hybrid nanoparticles as a positive MR contrast agent, Am. Chem. Soc., 128,15090-15091.
22. Jain, A., & Hirata, G.A. (2016). Photoluminescence, size and morphology of red-emitting Gd_2O_3:Eu^{3+} nanophosphor synthesized by various methods, Ceram. Int. 42, 6428–6435.
23. Jin, Y., Chen, S., Duan, J., Jia, G., & Zhang, J. (2015). Europium-doped Gd_2O_3 nanotubes cause the necrosis of primary mouse bone marrow stromal cells through lysosome and mitochondrion damage, J. Inorg. Biochem. 146, 28–36.

24. Ju, Q., Tu, D., Liu, Y., Li, R., Zhu, H., & Chen, J. (2011). Amine-functionalized lanthanide doped KGdF4 nanocrystals as potential optical/magnetic multimodal bioprobes, J. Am. Chem. Soc., 134, 1323-1330
25. Lechevallier, S.V., Lecante, P., Mauricot, R., Dexpert, H., Dexpert-Ghys J., & Kong, H.K. (2010). Gadolinium–Europium carbonate particles: controlled precipitation for luminescent biolabeling. Chem Mater., 22, 6153-6161.
26. Li, H., Wang, H., & Wang, L. (2013). Synthesis and sensing application of highly luminescent and water stable polyaspartate functionalized LaF3 nanocrystals, J. Mater. Chem. C, 1, 1105-1110.
27. Lin, S.L., Liu, T.Y., Lo, C.L., Wang, B.S., Lee, Y.J., Lin, K.Y., & Chang, A. (2016). Synthesis, surface modification, and photophysical studies of Ln_2O_2S: Ln^{3+}(Ln=Gd, Tb,Eu; Ln'=Tb and/or Eu) nanoparticles for luminescence bioimaging, J. Lumin., 175, 165–175.
28. Liu, X. J., Wang, C. Z., Hupalo, M., Yao, Y. X., Tringides, M. C., Lu, W. C., & Ho, K. M. (2010). Adsorption and growth morphology of rare-earth metals on grapheme studied by ab initio calculations and scanning tunnelling microscopy, Phys. Rev. B 82, 245408-245415.
29. Louis, C., Bazzi, R., Marquette, C. A., Bridot, J. L., Roux, S., & Ledoux, G. (2005). Nanosized hybrid particles with double luminescence for biological labelling, Chem Mater., 17, 1673–82.
30. Luo, W., Li, R., & Chen, X. (2009). Host-Sensitized Luminescence of Nd3+ and Sm3+ Ions Incorporated in Anatase Titania Nanocrystals, J. Phys. Chem. C, 113, 8772–8777.
31. Mahmoudi, M., Lynch, I., Ejtehadi, M. R., Monopoli, M. P., Bombelli, F. B., & Laurent, S. (2011). Protein−Nanoparticle Interactions: Opportunities and challenges, Chem. Rev., 111, 5610–5637.
32. Nichkova, M., Dosev, D., Gee, S. J., Hammock, B. D., & Kennedy, I. M. (2005). Microarrayimmunoassay for phenoxybenzoic acid using polymer encapsulated Eu: Gd2O3 nanoparticles as fluorescent labels, Anal.Chem., 77, 6864–6873.
33. Nichkova, M., Dosev, D., Gee, S. J., Hammock, B. D., & Kennedy, I. M. (2007). Quantum Dots as Reporters in Multiplexed Immunoassays for Biomarkers of Exposure to Agrochemicals, Anal. Lett.,40, 1423-1433.
34. Park, Y. I., Kim, J. H., Lee, K.T., Jeon, K-S., Na, H. B., & Yu, J. H. (2009). Nonblinking and nonbleaching upconverting nanoparticles as an optical imaging nanoprobe and T1magnetic resonance imaging contrast agent, Adv. Mater., 21, 4467-4471.
35. Que, Y., Feng, C., Lu, G., & Huang, X. (2017). Polymer-Coated Ultrastable and Biofunctionalizable Lanthanide Nanoparticles, ACS Applied Materials & Interfaces, 9, 14647−14655.
36. Rossner, W., & Grabmaier, B. C. (1991). Phosphors for X-Ray Detectors in Computed Tomography,) J. Lumin., 48, 29-36.
37. Sarkar, S., Chatti, M., & Mahalingam, V. (2014). Highly Luminescent Colloidal Eu3+-Doped KZnF3 Nanoparticles for the Selective and Sensitive Detection of CuII Ions, Chem. Eur. J., 20, 3311-3316.
38. Shi, H. Z., Li, L., Zhang, L.Y., Wang, T.T., Wang, C.G., & Su Z.M. (2015). Facile fabrication ofhollow mesoporous Eu^{3+}−doped Gd_2O_3nanoparticles for dual-modal imaging and drug delivery, Dyes Pigm. 123 8–15.
39. Stouwdam J. W., & van Veggel, F. C. J. M. (2002). Near-infrared emission of redispersible Er3+, Nd3+, and Ho3+ Doped LaF3, Nano Lett., 2, 733-737.
40. Sun, S.-J., Lin, K. H., Ju, S. P., & Li, J. Y. (2016), Electronic and structural properties of ultrathin molybdenum nanowires by density functional theory calculations. Sci. Adv. Mater., 8, 1648–1655.
41. Tissue, B.M. (1998). Synthesis and Luminescence of Lanthanide Ions in Nanoscale Insulating Hosts, Chem. Mater., 10, 2837-2845.
42. Tuo. W., Huayan, P., Rubiao, C., Dong, L., Hong, Z., Ye, S., Yanghui, L., & Le, W. (2016). Effect of solution pH value changes on fluorescence intensity of magnetic-luminescentFe3O4@Gd2O3:Eu3+nanoparticles, J. Rare Earths, 34 71–76.
43. Vashistha, N., Chandra A., & Singh, M. (2018). Influence of rhodamine B on interaction behaviour of lanthanide nitrates with 1st tier dendrimer in aqueous DMSO: A physicochemical, critical aggregation concentration and antioxidant activity study, J. Mol. Liq., 260, 323–341.

44. Wang, J., Li, Y., Patel, N. G., Zhang, G., Zhou, D., & Pang, Y. (2014). A single molecular probe for multi-analyte (Cr3+, Al3+ and Fe3+) detection in aqueous medium and its biological application, Chem. Commun., 50, 12258-12261.
45. Xiao, H., Li, P., Jia, F., & Zhang, L. (2009). General non aqueous sol–gel synthesis of nanostructured Sm2O3, Gd2O3, Dy2O3, and Gd2O3: Eu3+ Phosphor, J. Phys. Chem C., 113, 21034–21041.
46. Ye, Y., Lv, M., Zhang, X., & Zhang, Y. (2015). Colorimetric determination of copper (II) ions using gold nanoparticles as probe, RSC adv., 5, 102311-102317.
47. Zhang, J., Shade, C. M., Chengelis, D. A., & Petoud, S. (2007). A strategy to protect and sensitize near-infrared luminescent Nd3+ and Yb3+: organic tropolonate ligands for the sensitization of Ln(3+)-doped NaYF4 nanocrystals, J. Am. Chem. Soc. 129, 14834-14835.
48. Zhang, X., J. Xue, Ge, Y., Lei, B., Yan, D., Li, N., Liu, Z., Du, Y., & Cai, R. (2015). Controlled Synthesis of Ultrathin Lanthanide Oxide Nanosheets and Their Promising pH-Controlled Anticancer Drug Delivery, Chem. Eur. J., 21, 11954 – 11960.
49. Zhao, G., Tong, L., Cao, P., Nitz, M., & Winnik, M. A., (2014). Functional PEG–PAMAM-Tetraphosphonate Capped NaLnF4 Nanoparticles and their Colloidal Stability in Phosphate Buffer, Langmuir, 30, 6980-6989
50. Zhou, Y., Lin, J., & Wang, S. (2003). Energy Transfer and Up-Conversion Luminescence Properties of Y2O3:Sm and Gd2O3:Sm Phosphors, J. Solid State Chem., 171,391-395.
51. Zhou, Z., Yu, M., Yang, H., Huang, K., Li, F., Yi, T., & Huang, C. (2008). FRET-based sensor for imaging chromium (III) in living cells, Chem. Commun., 29, 3387-3389.
52. Zoua, H., Melro, L., Chaparro, T.C., de Souza Filho, I.R., Ananias, D., Lami, E.B., Santos, A.M., & Timmons, A.B. (2017). Adsorption study of a macro-RAFT agent onto SiO_2-coated Gd_2O_3:Eu^{3+}nanorods: requirements and limitations, Appl. Surf. Sci. 394, 519–527.

